

Segregated interactions in urban and online spaces

Xiaowen Dong,^{1,2†} Alfredo J. Morales,^{2,3†} Eaman Jahani,^{4†}
Esteban Moro,^{2,5} Bruno Lepri,⁶ Burcin Bozkaya,^{7,8}
Carlos Sarraute,⁹ Yaneer Bar-Yam,³ Alex ‘Sandy’ Pentland²

¹Department of Engineering Science, University of Oxford, Oxford, UK

²MIT Media Lab, Cambridge, MA, USA

³New England Complex Systems Institute, Cambridge, MA, USA

⁴MIT Institute for Data, Systems and Society, Cambridge, MA, USA

⁵Department of Mathematics and GISC, Universidad Carlos III de Madrid, Leganés, Spain

⁶Mobile and Social Computing Lab, Fondazione Bruno Kessler, Trento, Italy

⁷Behavioral Analytics & Visualization Lab, Sabanci University, Istanbul, Turkey

⁸New College of Florida, Sarasota, FL, USA

⁹Grandata Labs, Buenos Aires, Argentina

†These authors contributed equally to this work.

Urban income segregation is a widespread phenomenon that challenges societies across the globe. Classical studies on segregation have largely focused on the geographic distribution of residential neighborhoods rather than on patterns of social behaviors and interactions. In this study, we analyze segregation in economic and social interactions by observing credit card transactions and Twitter mentions among thousands of individuals in three culturally different metropolitan areas. We show that segregated interaction is amplified relative to the expected effects of geographic segregation in terms of both shopping activity and online communication. Furthermore, we find that seg-

regation increases with difference in socio-economic status but is asymmetric, i.e., the amount of interaction from poorer to wealthier neighborhoods is considerably larger than vice versa. Our results provide novel insights into the understanding of behavioral segregation in human interactions with significant socio-political and economic implications.

Introduction

Residential segregation has historically been associated with societal issues such as economic, educational, and health inequalities (1, 2); as a consequence, it has been a central focus in social, economic and political sciences (3–5). Recent studies show that while racial segregation seems to be decreasing in the United States (6, 7), income inequality has been simultaneously rising (8, 9). According to the Stanford Center on Poverty and Inequality, 1% of the American population held 21% of all the income in 2012, which is more than double of what they held in 1970 (8.4%). This change is coupled with a sharp increase in residential segregation by income (10). In forty years, the number of American families living in middle-income neighborhoods went from 65% down to 43% in large metropolitan areas. Families are thus increasingly living in either extremely poor or rich neighborhoods, endangering the existence and stability of the middle classes (11).

In order to quantify residential segregation, American census reports (12) calculate twenty different indexes across five dimensions, namely: *evenness*, *exposure*, *concentration*, *centralization* and *clustering* (13). These metrics are mostly based on static census data and do not reflect patterns in an activity or behavioral space. At the same time, regardless of whether they involve physical space or not, restrictions on any type of social interaction may be considered as forms of segregation (14). These, together with the increasing availability of data sources resulting from human activities (15, 16), have led to an increasing number of studies

on modern forms of segregation in spaces beyond residential neighborhoods. Most notably, recent works have shown that there exists clear separation between different ethnic or income groups in everyday activities such as visitation of urban areas (17–23) or consumption of online information (24–29), leading to the so-called “echo chambers” or “filter bubbles” (30).

While the literature mainly focuses on the limited exposure of certain socio-demographic and wealth groups to the others, the restriction on interactions between these groups (31) remains rather unexplored, possibly due to the lack of large-scale interaction data. The recent work of Morales *et al.* (23) has shown that groups of different income levels have differentiated topics of conversation, and that exposure limited by segregated interactions both offline and online is a key variable for homogeneization. Along a similar line of investigation, we combine in the present paper large-scale credit card transaction and Twitter data sets to study income segregation in daily shopping activities and online communication, thus capturing two explicit interactions in economic and social behavior. We analyze how the patterns of segregation in both offline and online activities are intertwined, and vary with respect to both difference in socio-economic status and geographical distance. We demonstrate the consistency in these patterns by examining different cultural and political contexts, in three large metropolitan areas from Europe, Latin America, and North America¹. Although we do not have a direct matching of individuals between the transaction and Twitter data sets, we study behaviors at the collective scale by aggregating the data by urban administrative neighborhoods, for which socio-economic status can be obtained from national census data.

The main contributions of the present paper are three-fold. First, we show that segregation in behavioral interactions is amplified with respect to the expected effect of geographic segregation, in terms of both shopping activity and online communication. Second, we analyse segregation with respect to socio-economic status and geographical distance, where we found

¹Credit card transaction data are only available for the European and Latin American cities.

that segregation is most pronounced between extreme income groups. Finally, we demonstrate that segregation is asymmetric, where the amount of interactions from poorer to wealthier neighborhoods is considerably larger than the other way around. These findings provide a new angle to study modern forms of segregated behavior, with implications on urban planning, policy-making, and inequality reduction.

Results

Human patterns of exploration in urban and social spaces are linked to both individual and regional economic growth (32–34). We measure exploration by means of the diversity of purchases and Twitter communication via mentions. In order to measure diversity, we first characterize each individual with a pair of vectors whose elements represent either shops (in the case of purchases) or other individuals (in the case of Twitter mentions), and count the number of times individuals purchase at each shop or communicate with other individuals, respectively. We then measure, as explained in Material and Methods, the individual diversity as the Shannon entropy of each vector. Figure 2 shows a scatter plot with the aggregate neighborhood diversity of purchases and Twitter mentions after averaging over the individuals who live in each neighborhood of the European (Figure 2(a)) and the Latin American cities (Figure 2(b)). The average neighborhood diversity of both types of behaviors are positively correlated with each other ($r = 0.45$ in Europe and $r = 0.38$ in Latin America), as well as with the neighborhood socio-economic status². This indicates that people living in poorer neighborhoods are less exploratory in their shopping and online activities, suggesting that they live in physically and virtually confined spaces.

²In the European city, the correlations between purchases and Twitter mentions' diversity and socio-economic status are $r = 0.72$ and $r = 0.38$, respectively; In the Latin American city, the correlations between purchases and Twitter mentions' diversity and marginalization index (negative socio-economic status) are $r = -0.70$ and $r = -0.33$, respectively; In the Northern American city, the correlation between Twitter mentions' diversity and median household income (approximation of socio-economic status) is $r = 0.40$.

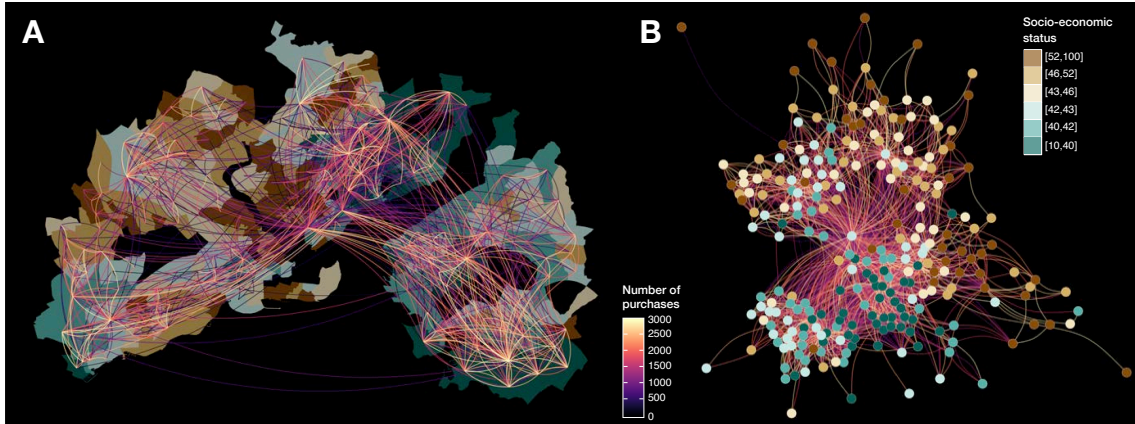


Figure 1: Purchase interactions among some of the neighborhoods in the European metropolitan area. Each neighborhood is shown as an area on the map (panel A) and as a node in a graph (panel B), and it is in both cases color-coded by its socio-economic status. Each curve in both panels represents an interaction between a pair of neighborhoods, and it is color-coded by the number of purchases made by residents of one neighborhood in another. The directions of the curves are represented by their convexity: curves of convex shape represent interactions from the left end point to the right end point, while those of concave shape represent interactions from right to left.

The confinement of physical and virtual spaces is associated with segregation by income. We analyze this relationship by creating networks of interactions among neighborhoods based on purchases and Twitter mentions. In both networks, nodes represent neighborhoods whose socio-economic status is obtained from census data. Edges represent either the number of purchases made by customers living in neighborhood i at stores in neighborhood j , or the number of tweets directed from users living in i to users living in j . Figure 1 displays an illustration of the purchase network for some of the neighborhoods in the European metropolitan area. By analyzing the structure of these networks and the distribution of edges among neighborhoods, we are able to observe patterns of urban mixing or segregation.

In order to quantify segregation, we group neighborhoods by socio-economic status and create mixing matrices whose elements show the aggregate number of interactions between every group of neighborhoods (35). We further normalize the mixing matrix for both behavior

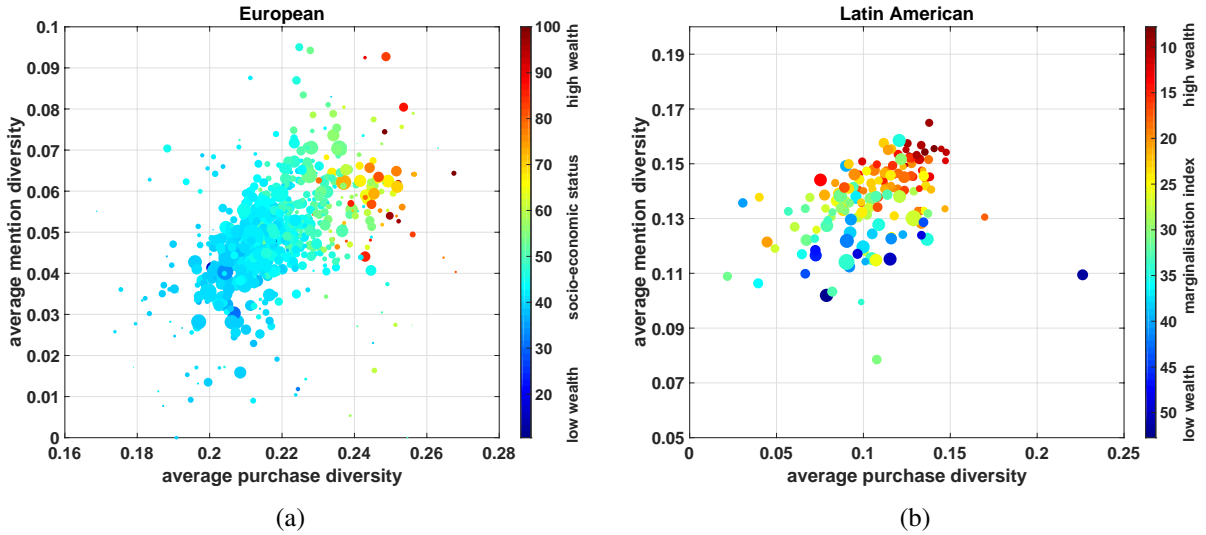


Figure 2: Neighborhood-level average diversity of purchases and Twitter mentions in the European and Latin American metropolitan areas. The size of the dots is proportional to the census population of the neighborhood and the color code indicates its wealth level. The correlation between both types of diversity is 0.45 and 0.38 for the European and Latin American case, respectively.

into a stochastic matrix whose elements show the probability of directed interaction among pairs of socio-economic groups (see Material and Methods and Appendix for the construction and visualization of the mixing matrices). We found that most of the interactions occur within groups of the same socio-economic status. We quantify such preference by calculating the assortativity coefficient of the mixing matrices (35). A coefficient of 1 indicates a perfectly assortative network while 0 indicates random mixing patterns³. The intuition is that assortative matrices are dominated by entries along and close to the matrix diagonal, indicating a stronger preference for neighborhoods to interact with similar ones (hence segregation). For example, in the European metropolitan area the assortativity coefficient of the mixing matrices for purchase and Twitter mentions is 0.43 and 0.35, respectively, indicating a certain degree of segregation

³A perfectly disassortative network, in which every edge connects two vertices of different types, has a negative coefficient generally in the range between -1 and 0 (35).

(see Figure S7(a) and Figure S7(b)).

While the assortativity coefficient shows a global description of the network, it misses heterogeneities in its structure, such as differences in the amount of segregation among certain socio-economic groups. In order to capture such heterogeneities, we analyze the segregation between the highest and lowest socio-economic strata and progressively include the remaining socio-economic groups in both directions until reaching the whole network. At each step, we define a threshold for the percentage of neighborhoods to be included (both at the top and bottom of the distribution) and measure their segregation with the assortativity coefficient (see Figure S10, Figure S11, and Figure S12 in Appendix). Figure 3(a) shows the assortativity coefficient as a function of the percentage of considered population at each extreme of the distribution, for both purchases and mentions' networks, in the European city. For comparison, we also include in the figure the expected results from two artificial networks generated by (i) simulating neighborhood-to-neighborhood interactions with a gravity-based model (36) and (ii) randomly reshuffling neighborhoods' socio-economic status in a null model (see Appendix for details on the construction of artificial interaction networks using gravity-based model and null model).

The following observations can be made from Figure 3(a). First, segregation is most pronounced between the highest and lowest socio-economic groups, which barely interact with each other, and decreases by including middle-class neighborhoods, which serve as “social bridges” between the richest and poorest parts of the society. Second, segregation in interactions (blue and orange) is stronger than the one expected from just geography (yellow and purple), implying that it cannot be simply attributed to the segregated distribution of residential households in the city. Third, this segregation is also stronger than the one produced by the null model (green and cyan) showing that the patterns we observe are significant and not an artifact of the data. While the segregation in shopping patterns could be expected partially given the

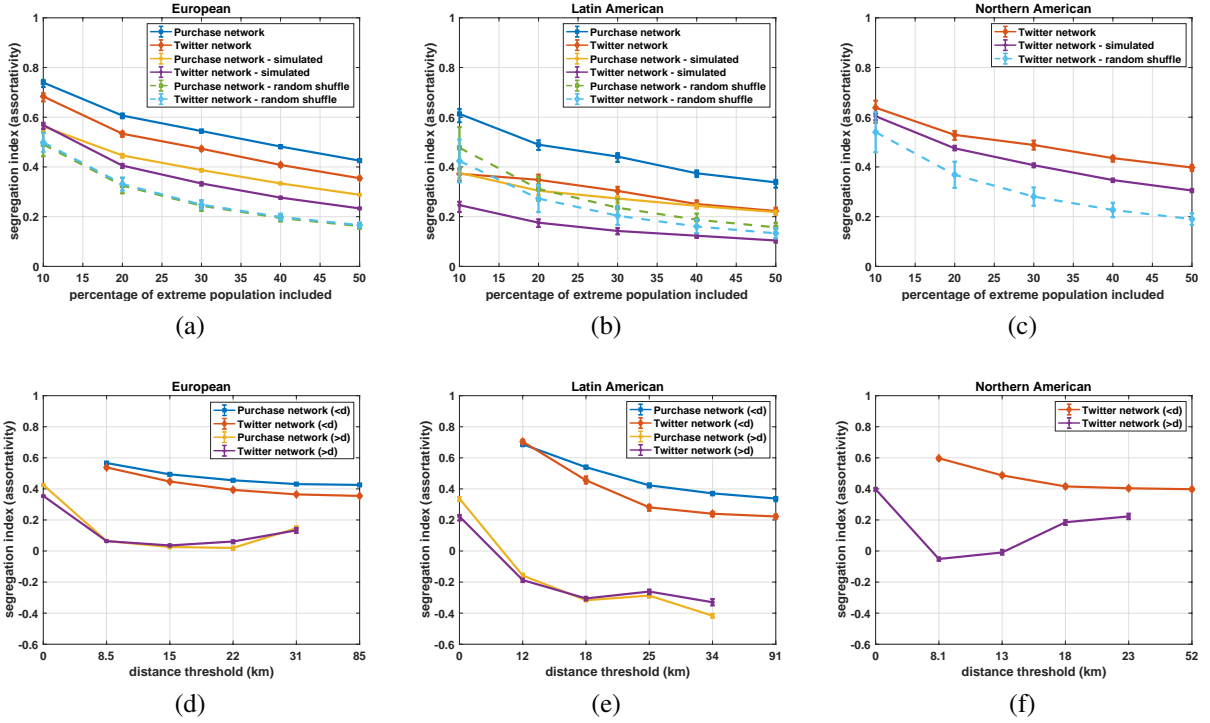


Figure 3: (Top) The assortativity for different networks, as a function of the percentage of population with extreme socio-economic status included in computation. (Bottom) The assortativity for different networks, as a function of the distance thresholds used for pruning edges in the interaction networks. The error bars in the green and cyan curves correspond to the standard deviations, and all other error bars correspond to the 95% confidence interval using a jackknife resampling technique as in (37).

limitations that prices impose on people, the fact that they also tend to self-segregate on the Internet is interesting. Similar patterns are also observed for the Latin and North American cities in Figure 3(b) and in Figure 3(c).

In order to further analyze the role of geography in the segregation in interactions, we measure the assortativity coefficient at multiple distances, by only considering subsets of neighborhood pairs that are either within a certain distance of d km or beyond this distance, representing short- and long-distance interactions, respectively (see Appendix for details on the analysis procedure). Figure 3(d-f) depicts the assortativity coefficients as a function of d for the empirical

networks for the three cities. It can be seen that both networks are predominately segregated due to short-distance interactions (blue and orange), with the network resulting from which having a consistently higher assortativity coefficient than that resulting from long-distance interactions (yellow and purple). In the case of purchases, short-distance interactions are less costly in terms of time and money, and are dominated by daily activities such as groceries or banking. Interestingly, the same pattern holds for online behaviors, which could be dominated by the interaction of local social groups and is consistent with the finding in (28). Moreover, the positive assortativity score for long-distance interactions in the European and North American cases (Figure 3(d,f)) suggests that self-segregation might even exist between neighborhoods that reside further away.

Apart from being segregated, interactions are not symmetric among different socio-economic groups. Poorer areas seem to interact more strongly with wealthier areas than the other way around. We measure this bias by looking at the excess of interactions directed from poorer to richer areas, relative to the number of interactions in the opposite direction. This is quantified as the difference between the sums of the lower and upper triangles of the mixing matrices. Figure 4 shows the poor-to-rich interaction bias as a function of the percentage of considered population (blue and orange), following the same methodology presented in Figure 3, where we initially consider only the highest and lowest extremes of the wealth distribution and progressively include neighborhoods towards the middle. The bias is always positive, and generally increases as we include the middle-low and middle-high wealth groups (with an exception in the case of the Northern American city). Moreover, although still presenting asymmetric interactions, the less bias from the lowest to the highest wealth group, together with the most pronounced segregation between these two groups as shown in Figure 3, indicates a polarization of behavior in this case.

We further investigate the robustness of the asymmetric relationship, by repeating the analy-

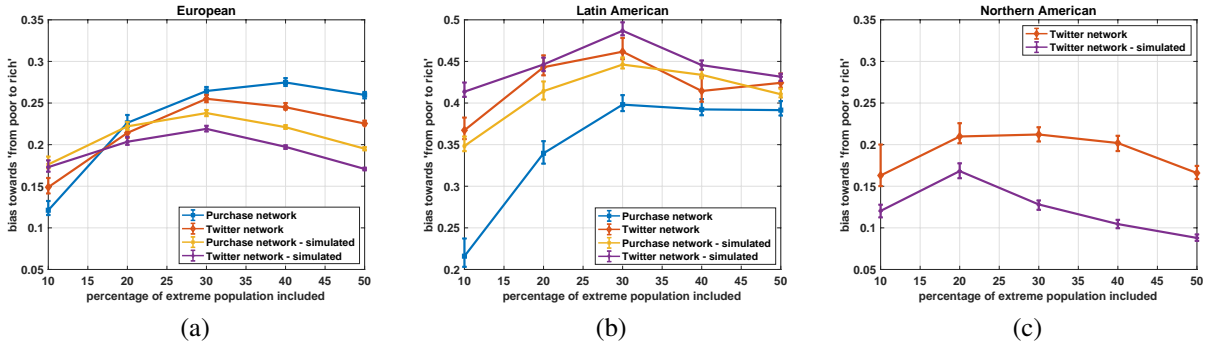


Figure 4: Asymmetry in the interaction patterns between the relatively poor and the relatively rich segments of the population. The error bars correspond to the 95% confidence interval using a jackknife resampling technique as in (37).

sis on the two artificial networks introduced before: (i) simulated interaction networks based on a gravity model, and (ii) the ones produced by randomly reshuffling the neighborhoods' socio-economic status in a null model. While in the former case the asymmetry persists (yellow and purple in Figure 4), it disappears in the latter where the bias drops to zero (see Figure S16, Figure S17 and Figure S18 in Appendix). For both the European and Northern American metropolitan areas, the observed asymmetric patterns in both offline and online behavior are more pronounced than than produced by the gravity-based model. This implies that, in these cases the stronger tendency of interactions from the relatively poor to the rich cannot be simply attributed to a geographical factor. The same argument, however, does not hold for the case of the Latin American city, which is likely due to the observation that richer neighborhoods account for more stores and Twitter users in that case (see Figure S2(b,c) in Appendix). Although the observed asymmetric relationship might be influenced by a larger number of stores and users (and popular ones) in richer neighborhoods, it nevertheless suggests that at macro scale there seems to exist a social hierarchy that is embedded in the behavioral interactions between different segments of the society.

Discussion

In summary, our results suggest that segregated patterns exist in both urban and online interactions between different socio-economic groups, and they seem stronger than that expected from merely the geographic distribution of residential households. While people might tolerate living close to neighborhoods of different socio-economic status, they prefer to interact, both physically and socially, with people from neighborhoods whose economic conditions are similar to their own. Such emerging behavior might be expected from purchase activities partially due to the constraints imposed by prices, but less so from online communication where boundaries are more likely self-imposed.

Indeed, while shopping behaviors are constrained by mobility, time and monetary resources associated with the spatial segregation patterns observed in our data, it was expected that online behavior would mitigate those constraints by creating a virtual *third-place* (38) where more diverse interaction would be possible. However, our results reinforce the recent findings that “echo chambers” in virtual space recreate and amplify the observed residential segregation in physical space. Nevertheless, it is still possible that segregation can be mitigated by encouraging virtual conversations and physical interactions between different groups. The promotion of such interactions might be critical in reducing segregation and prove more effective than simply an increase in the exposure to opposing views (29).

More interestingly, we observe that the restrictions on interactions, in both urban and online space, are most pronounced among the extremes of the wealth distribution, but fuzzy for the middle classes, which might act as social bridges (39) distributing information across the social system. Interactions across different segments of the society might therefore be promoted especially through the agency of groups with middle socio-economic status given their bridging roles. Furthermore, an asymmetric pattern of interaction seems to suggest the existence of a so-

cial hierarchy at macro scale, where richer areas attract not only an unequal amount of incoming money (see “Segregation and economic inequality” in Appendix) but also information. This, in turn, is crucial for the creation of new economic opportunities. As observed in Figure S19 and Figure S20, a stronger segregation pattern in purchase interactions is linked with a higher level of inequality between neighborhoods in terms of their sales revenue. This suggests that urban planners may consider a better strategy in allocating store locations for a more even distribution of capital, which can be achieved by promoting tax segmentation.

Our analysis has limitations. Even though the number of users in the two data sets are correlated (Figure S1(a) and Figure S2(a)), penetration rates of credit card and Twitter usage differ in neighborhoods of different socio-economic status. Richer neighborhoods tend to account for more samples in our data sets, an observation that is most pronounced for the Latin American city (Figure S2(b) and Figure S2(c)). This leads to under-representation of population in neighborhoods with lower socio-economic status. For both data sets, sampling bias could exist; furthermore, the credit card transaction data may only represent a fraction of the daily spending as people may choose to pay by cash in certain situations. Finally, our socio-economic status data are obtained at the neighborhood level, and may not necessarily reflect the economic situation of individuals in the data sets. Nevertheless, the general consistency between the results in three cities from three different continents across a period of several months suggests the validity of our findings in the contexts examined in the present study.

Materials and Methods

Data sets and pro-processing

The credit card transaction data sets are provided by two major financial institutions, one in an European country and one in a Latin American country. Each record in the data set corresponds to one credit card transaction along with customer and store IDs, as well as the time (day, hour

and minute) of the transaction and the spending amount in local currency. Additional information about the customers and stores are also made available, including customers' home location as well as store location and category. The customer-level data are appropriately anonymized such that each customer is represented by a pseudo-unique number and any unique identifier has been removed. The data are analyzed under legal restriction against re-identification, in a way that fully conforms to privacy laws of the two countries.

We focus our analysis on two large metropolitan areas of the two countries. As pre-processing steps, we first filter out foreign and online transactions to focus on local and physical activities. We then consider customers who made at least ten transactions in the data set. In the European case, this leads to a set of 2.4 million records of individual credit card purchases in a three-month period, made by 85 thousand individuals at 54 thousand stores. In the Latin American case, this consists of a set of 3.5 million records of individual credit card purchases in a four-month period, made by 200 thousand individuals at 55 thousand stores.

We collect geo-localized Twitter data sets using Twitter's Streaming API (40) during a similar period of the credit card data set for the European city and an extended 2-year period for the Latin and North American cities. In the European case, it contains 76 million geo-localized tweets within the metropolitan area of interest, from 1.4 million Twitter users. In the Latin American case, it contains 10.3 million geo-localized tweets within the metropolitan area under study, from 422 thousand Twitter users. Finally, in the Northern American metropolitan area, it consists of 22.4 million geo-localized tweets, from 862 thousand Twitter users.

On Twitter, a user A can mention or reply to another user B in his post in which case the post contains B's username. This allows us to build neighborhood-level Twitter mention networks. For this purpose, for the European case, we select a subset of 20.1 million tweets containing user mentions or replies that are posted by 1 million users, for whom we are also able to infer their home locations. For the Latin American and Northern American metropolitan areas, we

collect 3.8 million tweets and 8.1 million tweets containing user mentions or replies that are posted by 260 thousand and 440 thousand users, respectively.

It is worth noting that in this paper we study interactions among urban neighborhoods of different socio-economic status. In all the three metropolitan areas we consider, neighborhoods are administrative districts of varying sizes used for census purposes. We have around 660 such neighborhoods in the European case, around 160 in the Latin American case, and around 190 in the Northern American case. For the European city, the neighborhood-level socio-economic status is obtained from a recent census, which is a composite measure between 0 and 100 that quantifies the relative prosperity of the neighborhood based on a number of indicators such as income and education level. The higher the index, the more prosperous the neighborhood is. In the Latin American case, we use the neighborhood-level marginalization index from a recent census as an approximation of the (negative) socio-economic status, namely, the higher the marginalization index, the lower the socio-economic status. Finally, for the Northern American city, we use median household income from a recent national survey to approximate the socio-economic status of the neighborhoods.

Even though we do not have a matching between the individuals in the two different data sets, we are able to study both offline (purchases) and online (Twitter mentions) behavior at the level of administrative neighborhoods within the city. Specifically, we first associate the customers in the credit card data set as well as users in the Twitter data set with the neighborhoods in which they reside. We also associate the stores in the credit card data with the neighborhoods in which they are located. We then compute neighborhood-level interaction networks as described in the following sections.

Computation of the diversity score

For each individual s , we define the diversity as the Shannon entropy of his/her purchase (or Twitter) activities:

$$D(s) = - \sum_{t=1}^N p_{st} \log(p_{st}), \quad (1)$$

where p_{st} is the probability that an individual s (or Twitter user) visits a store t (or mentions another user t) and N is the total number of stores (or Twitter users). The average diversity score of a neighborhood is then defined as the average diversity of individuals living in that neighborhood. This approach is similar to the network-based approach of Eagle et al. (32).

Construction of the interaction networks

We construct two networks to capture interactions between different neighborhoods. In these networks, nodes represent neighborhoods and edges represent interactions whose intensities are captured by the weights of the edges. For purchase network, we define a directional edge from neighborhood i to j with weight $w_{ij}^{(p)}$, which is the number of purchases made by customers living in i at stores in j . Similarly, for Twitter mention network, we define a directional edge from neighborhood i to j with weight $w_{ij}^{(t)}$, which is the number of mentions made by Twitter users living in i to users in j .

Construction of the mixing matrices

To quantify segregation, we first construct the mixing matrices. Specifically, we divide all the neighborhoods into ten groups of equal size that have increasing socio-economic status from 1 to 10, i.e., the socio-economic status group for neighborhood i is $s(i) = [1, 2, \dots, 10]$. We then convert the original interaction networks into the 10 by 10 mixing matrices, whose mn -th entry

is defined as:

$$\begin{aligned} M_{mn}^{(p)} &= \sum_{s(i)=m, s(j)=n} w_{ij}^{(p)}, \\ M_{mn}^{(t)} &= \sum_{s(i)=m, s(j)=n} w_{ij}^{(t)}. \end{aligned} \quad (2)$$

Finally, we normalize the mixing matrix of both networks into a stochastic matrix:

$$\begin{aligned} S_{mn}^{(p)} &= \frac{M_{mn}^{(p)}}{\sum_n M_{mn}^{(p)}}, \\ S_{mn}^{(t)} &= \frac{M_{mn}^{(t)}}{\sum_n M_{mn}^{(t)}}. \end{aligned} \quad (3)$$

This way, $S_{mn}^{(p)}$ and $S_{mn}^{(t)}$ represent the probability of interaction from one socio-economic status group m to another n in terms of credit card purchases and Twitter mentions. The resulting mixing matrices for the interaction networks in the European, Latin American, and Northern American case are shown in Figure S7, Figure S8, and Figure S9, respectively.

Computation of the assortative mixing coefficient

Assortative mixing coefficient (or assortativity) is a measure proposed by Newman *et al.* (35) to quantify the phenomenon of homophily in social networks, which can also be used for measuring segregation in networks (41). In the context of the mixing matrices, it is equivalent to Cohen's Kappa, a classical psychometric measure of agreement on nominal variables (42). In our case, the more assortative the mixing matrices, the more segregated the behavioral interaction patterns.

The assortativity proposed in (35) is computed as follows. Given a weighted network, let e_{xy} be the fraction of weights of edges in the network that join nodes having attribute values x and y . The assortativity is then defined as:

$$r = \frac{\sum_{xy} xy(e_{xy} - a_x b_y)}{\sigma_x \sigma_y}, \quad (4)$$

where $\sum_{xy} e_{xy} = 1$, $a_x = \sum_y e_{xy}$ is the fraction of weights of edges starting from nodes with attribute value x , $b_y = \sum_x e_{xy}$ is the fraction of that connecting to nodes with attribute value y , and

$$\sigma_x = \sqrt{\sum_x x^2 a_x - \left(\sum_x x a_x\right)^2} \quad (5)$$

and

$$\sigma_y = \sqrt{\sum_y y^2 b_y - \left(\sum_y y b_y\right)^2} \quad (6)$$

are the standard deviations of distributions of a_x and b_y , respectively. As we can see, the assortativity r is the Pearson correlation coefficient between the attributes of the two end nodes for all the edges.

In Appendix, we describe in detail how we compute the assortativity based on subset of socio-economic status groups as well as geographical distance between neighborhoods.

Acknowledgements

The authors would like to thank the European bank as well as the American company who donated the credit card transaction data sets for this research.

References

1. http://web.stanford.edu/~mrosenfe/urb_notes_effects_segregation.htm (2013). Accessed: 2019-03-17.
2. R. J. Sampson, *University of Chicago Press* (2012).
3. E. W. Burgess, *The Annals of the American Academy of Political and Social Science* **140**, 105 (1928).
4. O. D. Duncan, B. Duncan, *American Sociological Review* **20**, 210 (1955).

5. T. C. Schelling, *The Journal of Mathematical Sociology* **1**, 143 (1971).
6. E. Glaeser, J. Vigdor, *Manhattan Institute for Policy Research* (2012).
7. G. Firebaugh, C. R. Farrell, *Demography* **53**, 139 (2016).
8. S. F. Reardon, K. Bischoff, *American Journal of Sociology* **116**, 1092 (2011).
9. R. Florida, C. Mellander, *Regional Studies* **50**, 79 (2016).
10. R. Fry, P. Taylor, *Pew Research Center* (2012).
11. <http://inequality.stanford.edu/income-segregation-maps> (2018).
Accessed: 2019-03-17.
12. J. Iceland, D. H. Weinberg, E. Steinmetz, *U.S. Census Bureau, Series CENSR-3* (2002).
13. D. S. Massey, N. A. Denton, *Social Forces* **67**, 281 (1998).
14. L. Freeman, *Sociological Methods & Research* **6**, 411 (1978).
15. D. Lazer, *et al.*, *Science* **323**, 721 (2009).
16. A. Pentland, *Penguin Press* (2014).
17. D. W. S. Wong, S.-L. Shaw, *Journal of Geographical Systems* **13**, 127 (2011).
18. N. Bora, Y.-H. Chang, R. Maheswaran, *Proceedings of the International Conference on Social Computing, Behavioral-Cultural Modeling, and Prediction* (2014), pp. 11–18.
19. W. R. Boterman, S. Musterd, *Cities* **59**, 139 (2016).
20. D. Wang, F. Li, *Cities* **59**, 148–155 (2016).
21. N. M. Yip, R. Forrest, S. Xian, *Cities* **59**, 156 (2016).

22. Q. Wang, N. E. Phillips, M. L. Small, R. J. Sampson, *Proceedings of the National Academy of Sciences* (2018).
23. A. J. Morales, X. Dong, Y. Bar-Yam, A. Pentland, *Royal Society Open Science* **6**, 190573 (2019).
24. M. Gentzkow, J. M. Shapiro, *The Quarterly Journal of Economics* **126**, 1799 (2011).
25. A. J. Morales, J. Borondo, J. C. Losada, R. M. Benito, *Chaos* **25**, 033114:1 (2015).
26. E. Bakshy, S. Messing, L. Adamic, *Science* **348**, 1130 (2015).
27. W. Quattrociocchi, A. Scala, C. R. Sunstein, *Available at SSRN: <http://ssrn.com/abstract=2795110>* (2016).
28. M. T. Bastos, D. Mercea, A. Baronchelli, *arXiv:1709.05233* (2017).
29. C. A. Bail, *et al.*, *Proceedings of the National Academy of Sciences* (2018).
30. G. Levy, R. Razin, *Annual Review of Economics* **11**, 303 (2019).
31. J. Blumenstock, L. Fratamico, *Proceedings of the 4th Annual Symposium on Computing for Development* (2013).
32. N. Eagle, M. Macy, R. Claxton, *Science* **328**, 1029 (2010).
33. V. K. Singh, B. Bozkaya, A. Pentland, *PLOS ONE* **10**, e0136628 (2015).
34. X. Dong, *et al.*, *International Conference on Computational Social Science* (2016).
35. M. E. J. Newman, *Physical Review E* **67**, 026126 (2003).
36. G. Krings, F. Calabrese, C. Ratti, V. D. Blondel, *Journal of Statistical Mechanics: Theory and Experiment* **L07003** (2009).

37. B. Efron, *SIAM Review* **21**, 460 (1979).
38. <http://www.pewinternet.org/2001/10/31/online-communities> (2001). Accessed: 2019-03-17.
39. X. Dong, *et al.*, *ACM Transactions on Intelligent Systems and Technology, Special Issue on Urban Intelligence* **9**, 33:1 (2018).
40. <https://developer.twitter.com/en/docs/tweets/filter-realtime/guides/basic-stream-parameters.html> (2019). Accessed: 2019-03-17.
41. A. Rodriguez-Moral, M. Vorsatz, *Complex Networks and Dynamics*, P. Commendatore, M. Matilla-García, L. M. Varela, J. S. Cánovas, eds. (Springer, Cham, 2016), pp. 93–119.
42. M. Bojanowskia, R. Corten, *Social Networks* **39**, 14–32 (2014).
43. J. Greenwood, N. Guner, G. Kocharkov, C. Santos, *American Economic Review* **104**, 348 (2014).
44. T. Louail, M. Lenormand, J. M. Arias, J. J. Ramasco, *Applied Network Science* **2** (2017).

Appendix

Data statistics

Figure S1(a) and Figure S2(a) illustrate the comparison between the number of credit card customers and Twitter users in the European and in the Latin American cases, respectively. In both figures, the color code indicates the socio-economic status of the neighborhoods. We see that, for both metropolitan areas, the number of people in the two data sets are correlated ($r = 0.76$ in the European case and $r = 0.69$ in the Latin America case). The other plots in

Figure S1, Figure S2 and Figure S3 show the relationship between the number of credit card users as well as the one of Twitter users in each neighborhood, and the neighborhood-level socio-economic index. As expected, the number of users in both data sets are positively correlated with neighborhood-level socio-economic index, an association that is most pronounced in the case of the Latin American metropolitan area.

Figure S4 shows the distributions of the number of credit card customers, stores, Twitter users, and of the socio-economic status of the neighborhoods in the European metropolitan area, where Figure S5 shows the same distributions in the Latin American metropolitan area. Finally, Figure S6 shows the distributions of the number of Twitter users and of the median household income for the neighborhoods in the Northern American metropolitan area.

Computation of assortativity based on subset of socio-economic status groups

We propose the following framework for analyzing segregation among groups of neighborhoods of different socio-economic status. We first consider only entries in $M_{mn}^{(p)}$ and $M_{mn}^{(t)}$ that correspond to groups 1 and 10 (those of lowest and highest wealth), and normalize the resulting 2 by 2 matrices as described above to obtain the mixing matrices that correspond to only these two socio-economic status groups (shown in the first column of Figure S10, Figure S11 and Figure S12). We then compute the assortativity of these mixing matrices. Next, we include groups 2 and 9, and compute the 4 by 4 mixing matrices as well as the assortativity. This process is repeated until we eventually include all socio-economic status groups. The mixing matrices at each step are shown in the different columns of Figure S10, Figure S11 and Figure S12 for the European, Latin American, and Northern American cases, respectively. These are the matrices based on which we produce the results shown in Figure 3.

Computation of assortativity based on geographical distance

For analyzing interaction patterns between neighborhood pairs of different geographical distances, we propose the following framework. We first prune the interaction networks by removing edges that correspond to neighborhood pairs of distance smaller or larger than a set of thresholds. We then compute the assortativity that corresponds to the networks with the remaining subset of edges.

The distance thresholds are chosen to be the 20, 40, 60, 80, and 100 percentiles of a vector containing all the pairwise distances, which are 8.5km, 15km, 22km, 31km and 85km in the European case, 12km, 18km, 25km, 34km and 91km in the Latin American case, and 8.1km, 13km, 18km, 23km and 52km in the Northern American case. These thresholds are generally consistent across the three metropolitan areas.

The results are shown in Figure 3(d), Figure 3(e) and Figure 3(f). It is natural to see that keeping edges greater than 0km (yellow and purple curves in Figure 3(d)) is equivalent to removing edges greater than 85km (blue and orange curves in Figure 3(d)), which is the maximum distance between any pair of neighborhoods.

Construction of simulated interaction networks using a gravity-based model

To illustrate the difference between the empirical interaction patterns and the one that would have been caused by geographic distribution of neighborhoods, we simulate offline and online interaction networks between neighborhoods by considering the following model similar to the gravity-based model considered in (36):

$$\begin{aligned}
 w_{ij}^{(p)} &\approx c_p \frac{[n_i^{(p)}]^{\beta_{p1}} [m_j^{(p)}]^{\beta_{p2}}}{[T_{ij} + \epsilon_p]^{\alpha_p}}, \\
 w_{ij}^{(t)} &\approx c_t \frac{[n_i^{(t)}]^{\beta_{t1}} [m_j^{(t)}]^{\beta_{t2}}}{[T_{ij} + \epsilon_t]^{\alpha_t}},
 \end{aligned} \tag{7}$$

where $w_{ij}^{(p)}$ and $w_{ij}^{(t)}$ are the empirically observed edge weights in the purchase and Twitter networks, respectively, $n_i^{(p)}$ and $n_i^{(t)}$ are the numbers of credit card customers and Twitter users in neighborhood i , respectively, and T_{ij} is the geographical distance between the centroids of the neighborhoods i and j .

We obtain optimal values for the parameters $c_p, \beta_{p1}, \beta_{p2}, \epsilon_p, \alpha_p, c_t, \beta_{t1}, \beta_{t2}, \epsilon_t$ and α_t by fitting a weighted Ordinary Least Squares (OLS) model to the observed number of purchases $w_{ij}^{(p)}$ or mentions $w_{ij}^{(t)}$, where we weight the fitting for $w_{ij}^{(p)}$ or $w_{ij}^{(t)}$ with its own value:

$$\begin{aligned} \log w_{ij}^{(p)} &\approx (\log c_p + \beta_{p1} n_i^{(p)} + \beta_{p2} m_j^{(p)} - \alpha_p (T_{ij} + \epsilon_p)) \times w_{ij}^{(p)}, \\ \log w_{ij}^{(t)} &\approx (\log c_t + \beta_{t1} n_i^{(t)} + \beta_{t2} m_j^{(t)} - \alpha_t (T_{ij} + \epsilon_t)) \times w_{ij}^{(t)}. \end{aligned} \quad (8)$$

In the European, Latin American and Northern American cases, the values of the parameters are shown in Table S1(a), Table S1(b) and Table S1(c), respectively, and the fitting for the two interaction networks in each country is shown in Figure S13, Figure S14 and Figure S15, respectively.

Upon obtaining these parameters, we compute simulated number of purchases and mentions $\hat{w}_{ij}^{(p)}$ and $\hat{w}_{ij}^{(t)}$ using the right hand side of Equation (7). We then use these simulated networks to compute the segregation index (assortativity) according to the gravity-based model. The results are shown in Figure 3(a), Figure 3(b), and Figure 3(c) for the European, Latin American, and Northern American cases, respectively.

Construction of artificial interaction networks using a null model

We further validate the observed segregation pattern by comparing it against the one produced by a null model, in which socio-economic status of the neighborhoods are randomized to leave only the segregation effect of individuals visiting stores or mentioning others in their home neighborhoods. Specifically, we first randomly shuffle the socio-economic status of the neighborhoods. We then re-compute the artificial interaction networks for both offline purchases and

online Twitter mentions. Finally, we compute the segregation index (assortativity) according to the null model. The results are shown in Figure 3(a), Figure 3(b), and Figure 3(c) for the European, Latin American, and Northern American cases, respectively.

The jackknife resampling

To test the sensitivity of the assortativity of the interaction networks to certain edges, we use the jackknife resampling technique originally proposed in (37) and then adopted in (35). The idea is to randomly remove a certain percentage (5% in our case) of edges in each network, and then re-compute the assortativity of the network. For all the results shown in Figure 3, we apply the jackknife resampling for 100 times, and compute the 95% confidence interval of the assortativity.

Segregation and economic inequality

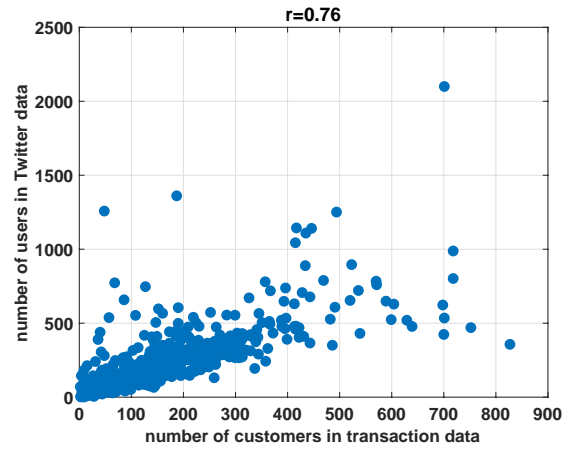
Segregation by income has direct implications on emerging economic inequalities, such as the unequal flow of money in the city (43). We investigate this relationship by analyzing the flow of money in the city using the purchase behavior of individuals and the distribution of sales revenue across neighborhoods. To this end, we add up the sales revenue of all the stores in each neighborhood, and compute the GINI coefficient of the resulting distribution across neighborhoods, similarly to the previous study in (44). The GINI coefficient can be thought of as an approximation of the economic inequality between the neighborhoods, which is then analyzed together with the assortativity (segregation index).

In addition to the empirical purchase networks, we repeat the same analysis on two artificial networks: (i) simulated purchase networks based on a gravity model and (ii) the ones produced by randomly reshuffling the location (in terms of neighborhood) of a fraction of the stores as well as customer homes in a null model. For the simulated network based on the gravity model,

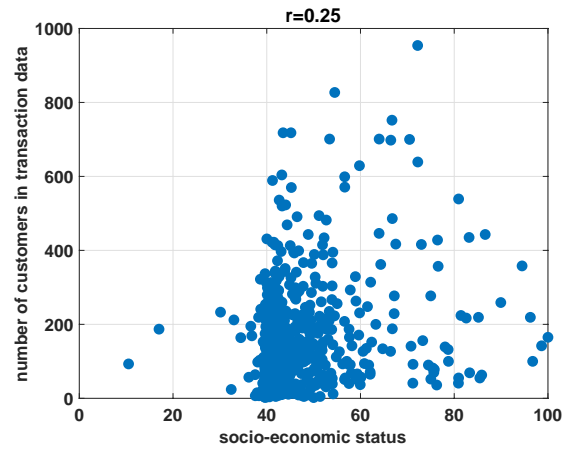
we adjust each transaction amount from neighborhood i to j by multiplying the actual amount with the ratio of the actual number of transactions from i to j to the simulated one, and then compute neighborhood-level sales revenue in the same way. Finally, we compute the GINI coefficient as well as the assortativity corresponding to this network.

For the networks based on random reshuffling, we use five fractions (i.e., 20%, 40%, 60%, 80% and 100%) for the reshuffling procedure. It is worth noting that such reshuffling does not change the number of customers and stores in each neighborhood nor the amount for each transaction, but only breaks the segregation pattern in purchase behavior. For each fraction, we apply the random reshuffling procedure for 50 times to compute the standard deviation of the resulting GINI coefficient and assortativity.

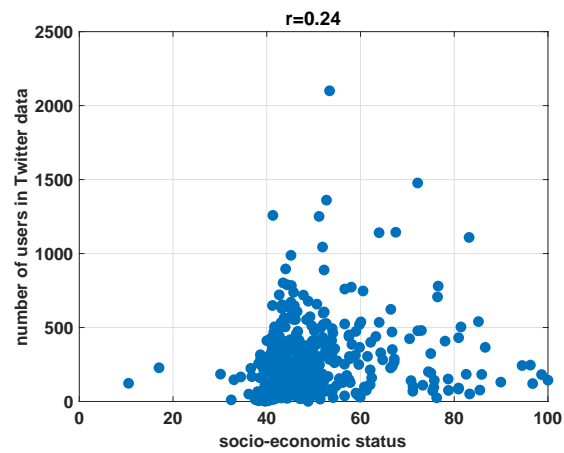
In Figure S19 and Figure S20 we present the GINI coefficient as a function of the assortativity for the empirical purchase network, the gravity model simulated network, and five networks based on random reshuffling of the customer and store locations. As we can see, inequality and segregation are highest in the empirical case, while in the gravity model they drop about 17% and 33%, respectively. As we reshuffle the location of stores and customers, both the GINI coefficient and the assortativity decrease. However, while segregation goes all the way down to zero, a considerable degree of inequality persists. This is due to the inhomogeneous number of stores across neighborhoods. In summary, these results show that a stronger segregation pattern in purchase behavior is linked with a higher level of inequality between neighborhoods in terms of their sales revenue.



(a)

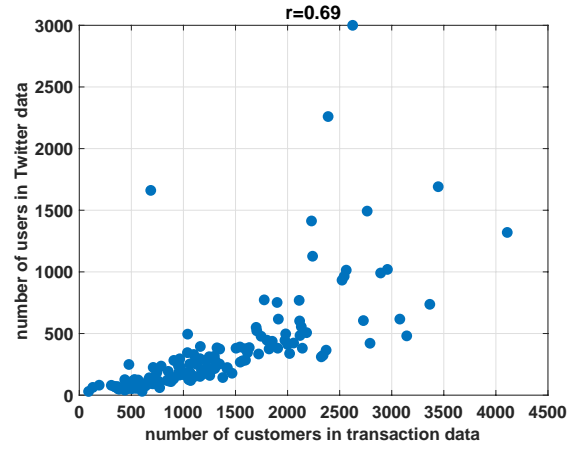


(b)

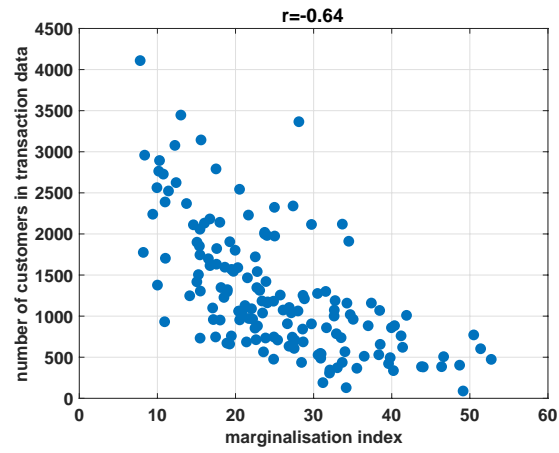


(c)

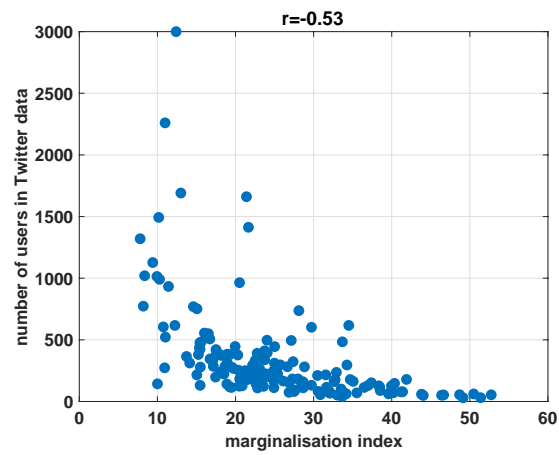
Figure S1: The relationship between the number of customers in the transaction data set, the number of users in the Twitter data set, and the neighborhood-level wealth, for the European metropolitan area.



(a)



(b)



(c)

Figure S2: The relationship between the number of customers in the transaction data set, the number of users in the Twitter data set, and the neighborhood-level wealth, for the Latin American metropolitan area.

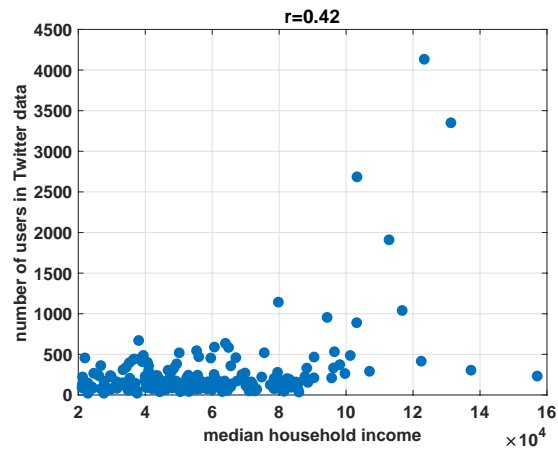


Figure S3: The relationship between the number of users in the Twitter data set and the neighborhood-level wealth, for the Northern American metropolitan area.

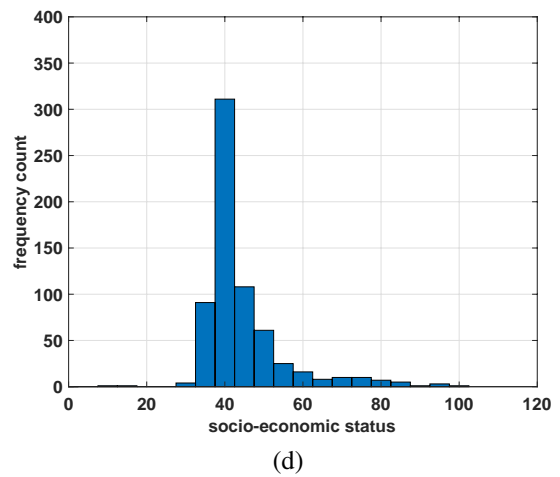
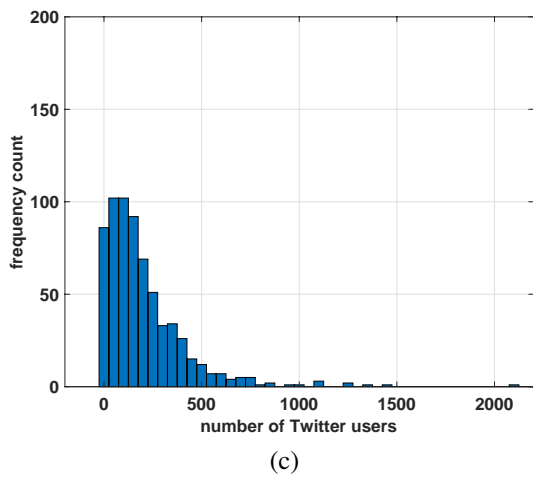
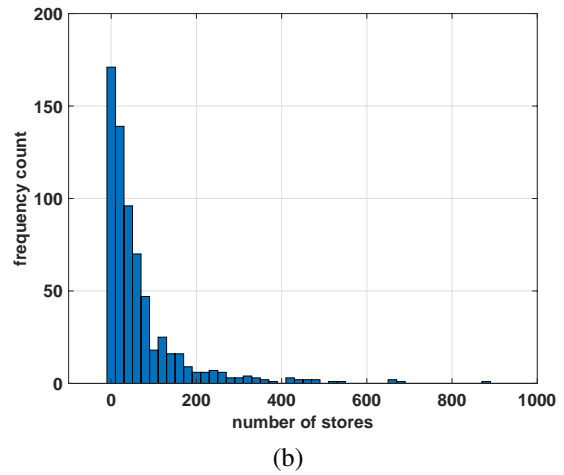
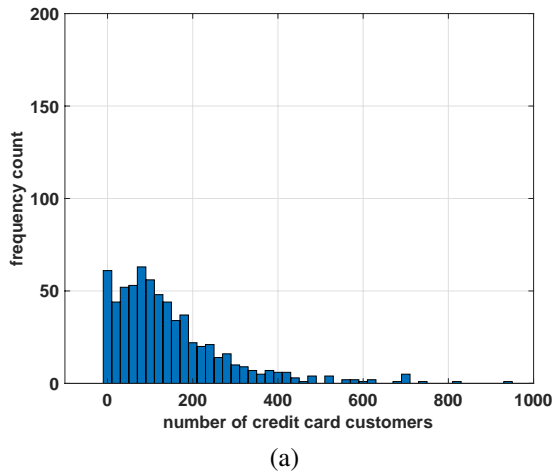
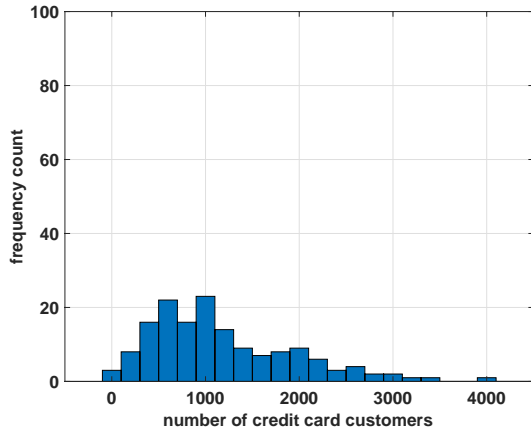
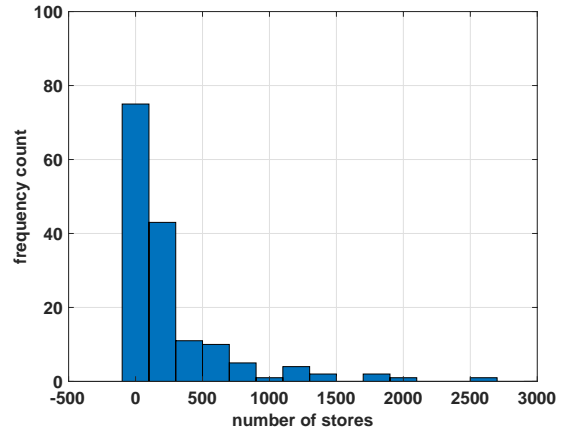


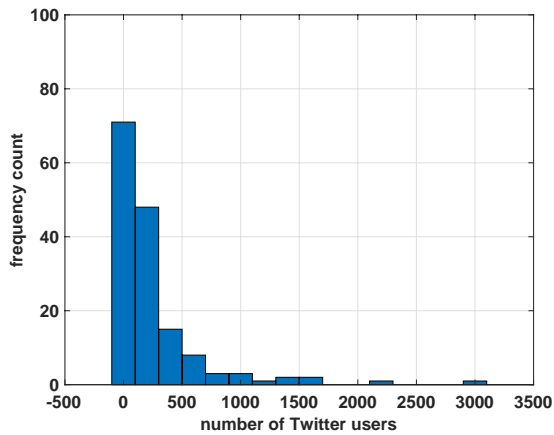
Figure S4: Histograms of (a) the number of credit card customers, (b) the number of stores, (c) the number of Twitter users, and (d) the socio-economic status, for neighborhoods in the European metropolitan area.



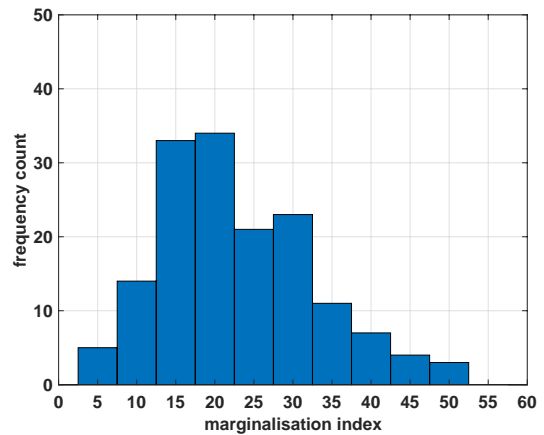
(a)



(b)

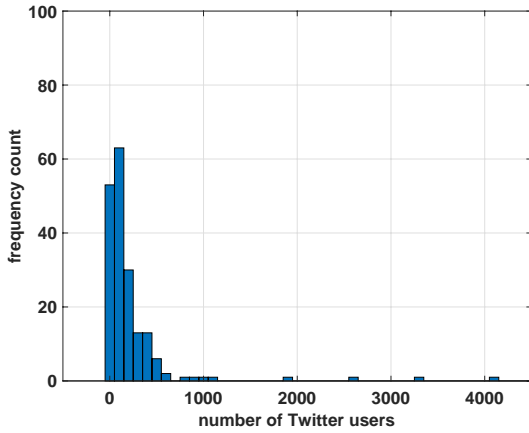


(c)

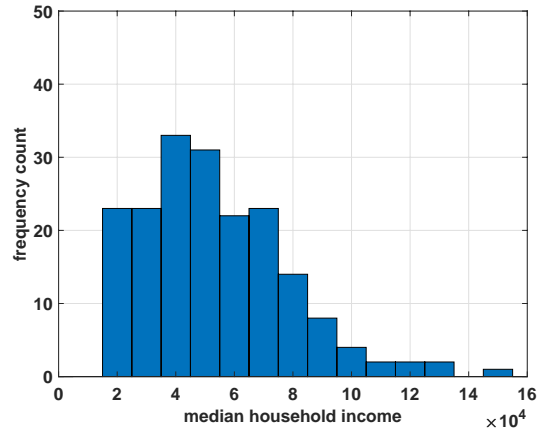


(d)

Figure S5: Histograms of (a) the number of credit card customers, (b) the number of stores, (c) the number of Twitter users, and (d) the socio-economic status, for neighborhoods in the Latin American metropolitan area.

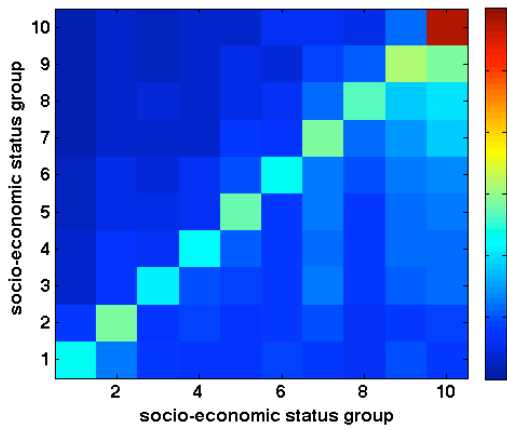


(a)

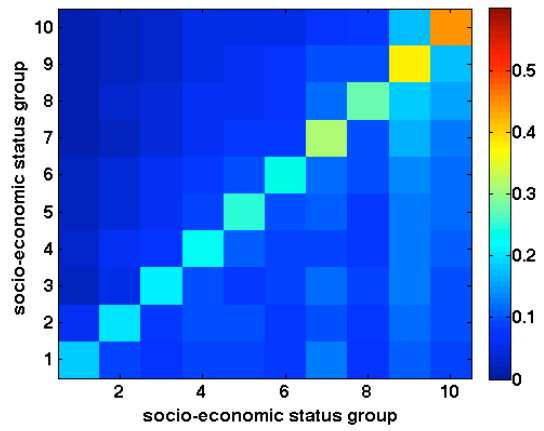


(b)

Figure S6: Histograms of (a) the number of Twitter users, and (b) the median household income, for neighborhoods in the Northern American metropolitan area.



(a)



(b)

Figure S7: Mixing matrices for (a) the purchase network and (b) the Twitter mention network, for ten socio-economic status groups in the European metropolitan area. Socio-economic status groups are ordered from the lowest wealth (1) to the highest wealth (10).

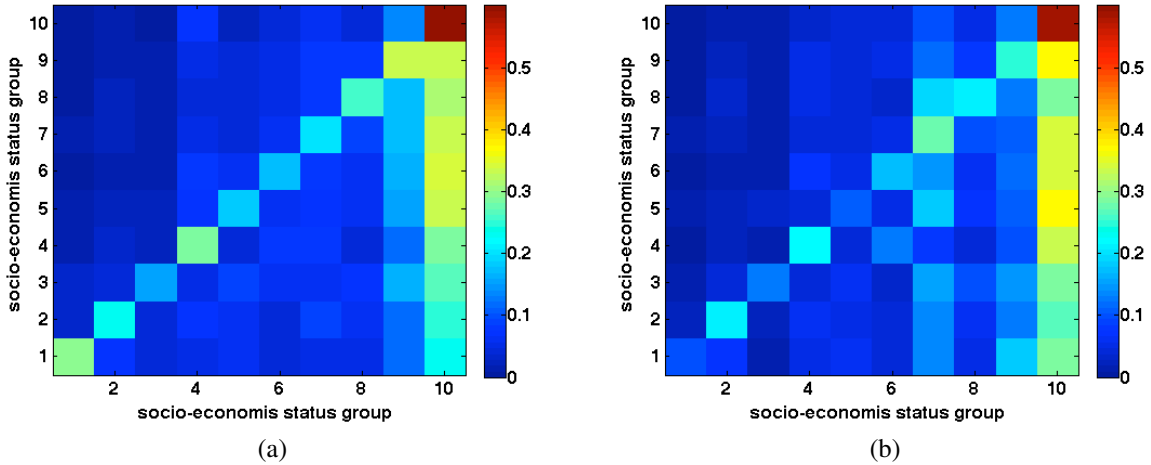


Figure S8: Mixing matrices for the (a) purchase network and (b) mention network, for ten socio-economic status groups, in the Latin American metropolitan area. Socio-economic status groups are ordered from the lowest wealth (1) to the highest wealth (10).

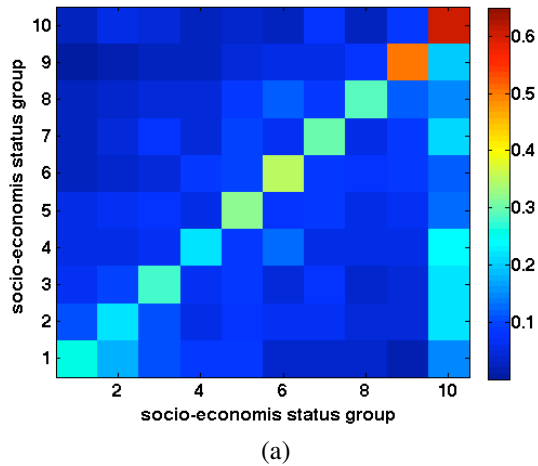


Figure S9: Mixing matrix for the mention network, for ten income groups, in the Northern American metropolitan area. Socio-economic status groups are ordered from the lowest wealth (1) to the highest wealth (10).

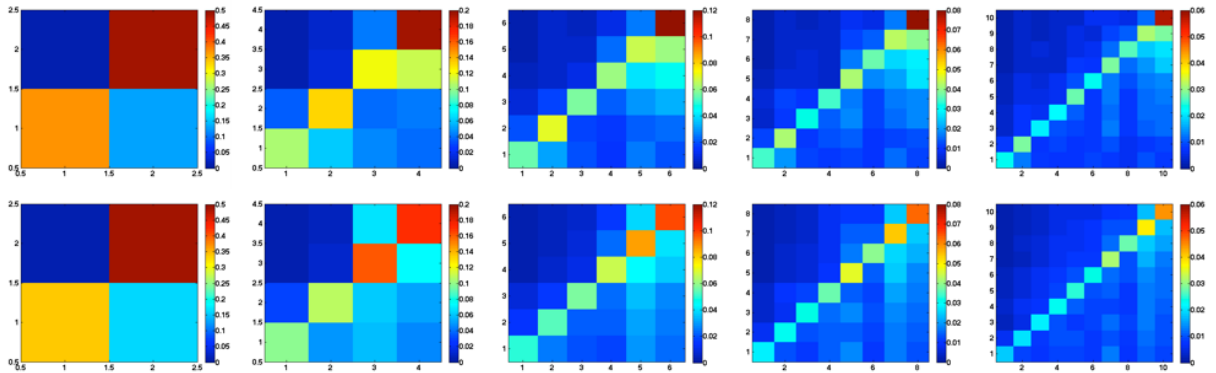


Figure S10: Mixing matrices of (Top) purchase and (Bottom) Twitter mention networks for extreme population in terms of socio-economic status group for the European metropolitan area. The columns from left to right correspond to 1, 2, 3, 4 and 5 extreme groups on both the poor and the rich sides.

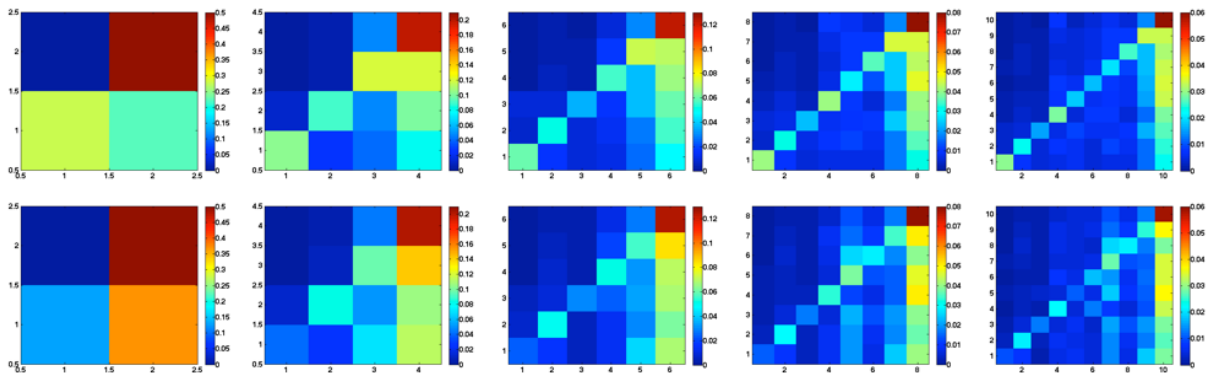


Figure S11: Mixing matrices of (Top) purchase and (Bottom) Twitter mention networks for extreme population in terms of socio-economic status group for the Latin American metropolitan area. The columns from left to right correspond to 1, 2, 3, 4 and 5 extreme groups on both the poor and the rich sides.

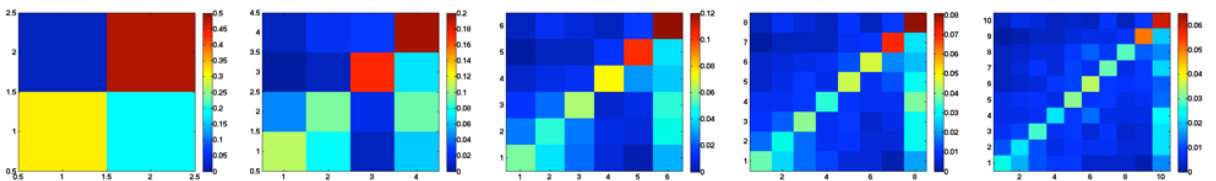
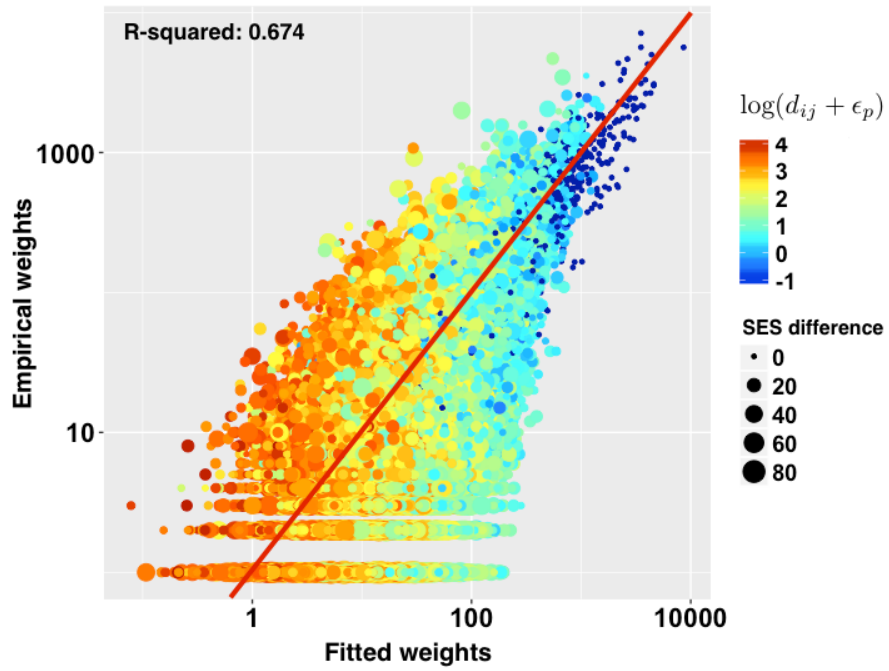
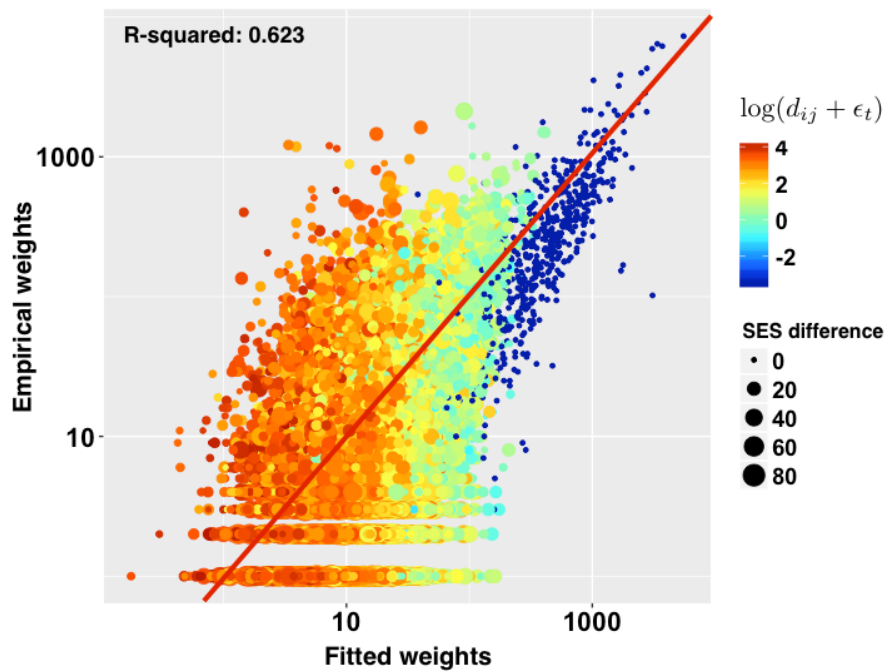


Figure S12: Mixing matrices of Twitter mention networks for extreme population in terms of median household income for the Northern American metropolitan area. The columns from left to right correspond to 1, 2, 3, 4 and 5 extreme groups on both the poor and the rich sides.

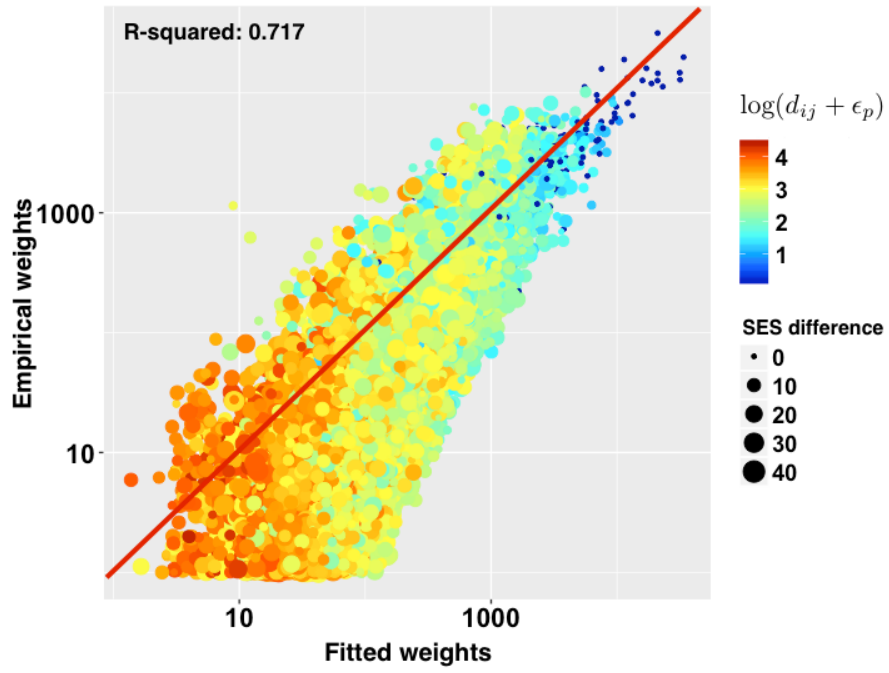


(a)

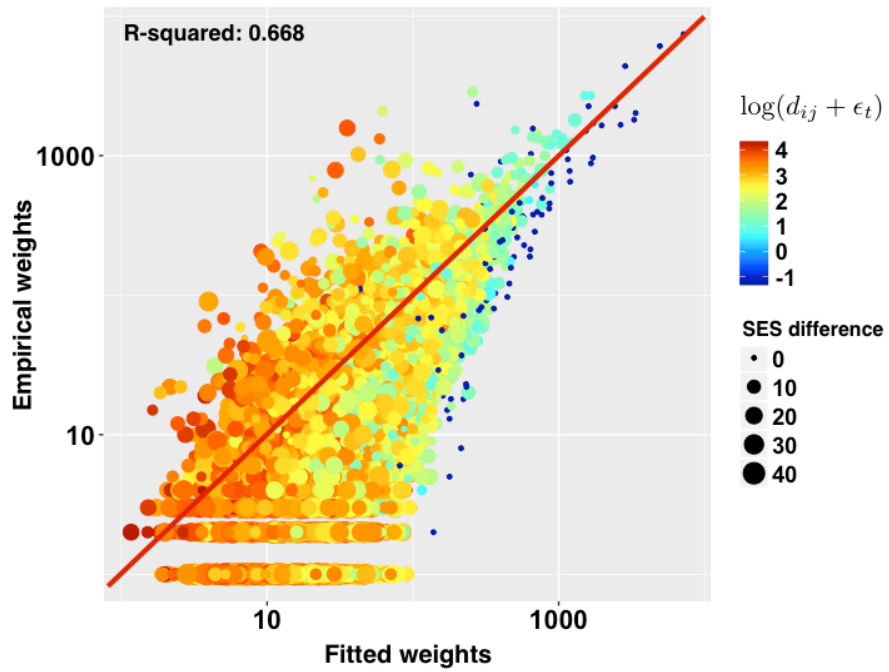


(b)

Figure S13: Weighted OLS fitting for (a) number of purchases and (b) number of mentions, for the European metropolitan area.



(a)



(b)

Figure S14: Weighted OLS fitting for (a) number of purchases and (b) number of mentions, for the Latin American metropolitan area.

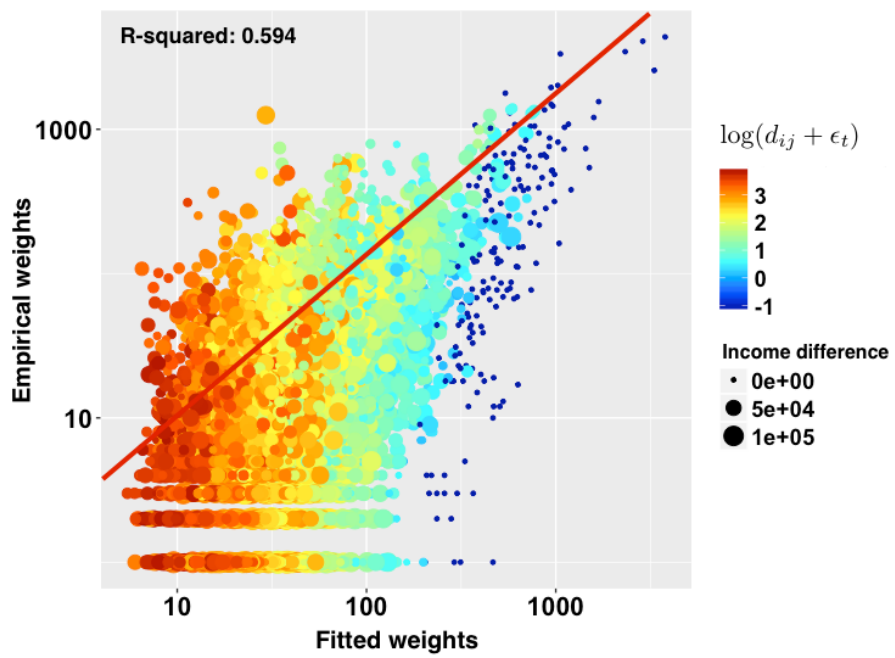


Figure S15: Weighted OLS fitting for number of mentions, for the Northern American metropolitan area.

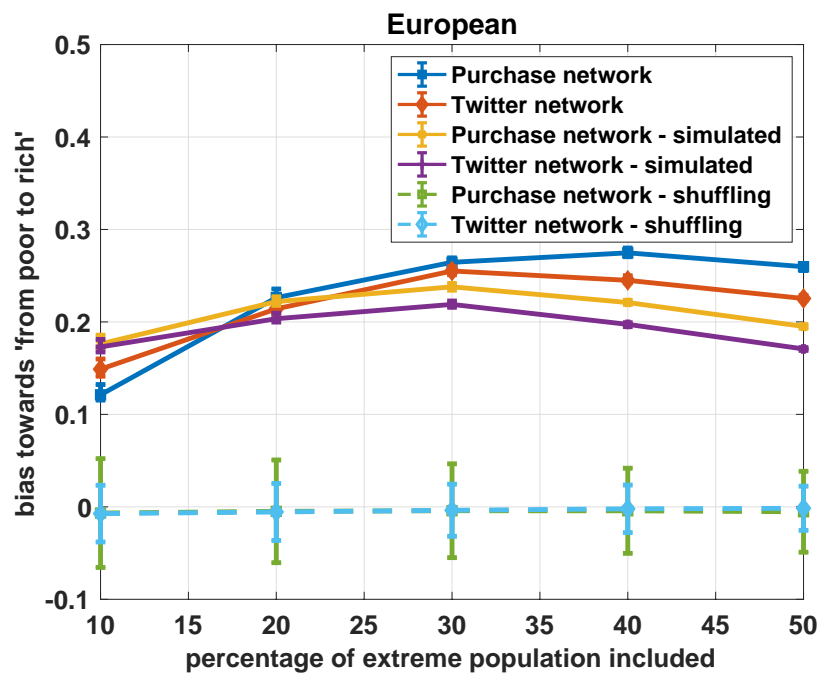


Figure S16: Asymmetry in the interaction patterns between the relatively poor and the relatively rich segments of the population in the European metropolitan area. The error bars in the curves for the random shuffling case correspond to the standard deviations, and all the other error bars correspond to the 95% confidence interval using a jackknife resampling technique as in (37).

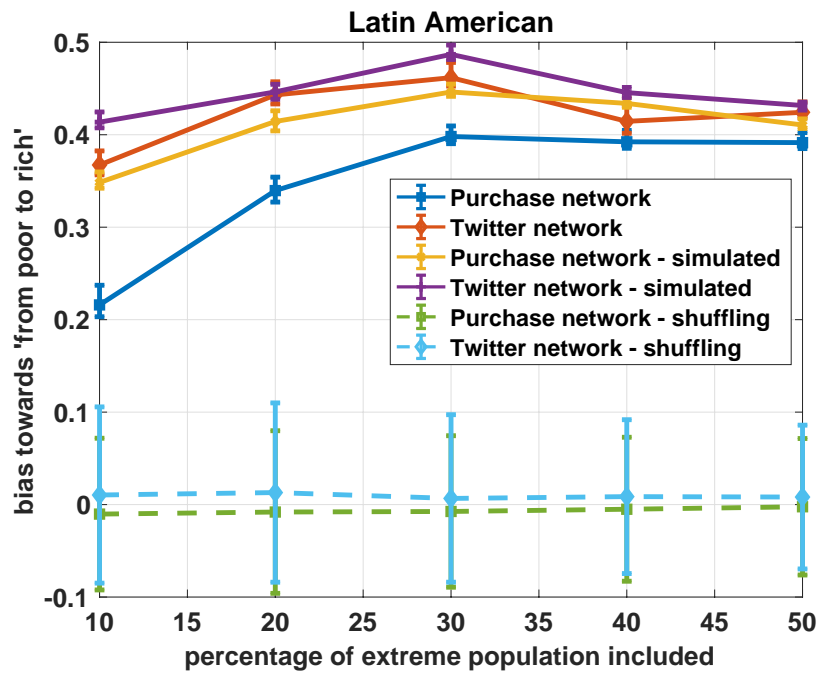


Figure S17: Asymmetry in the interaction patterns between the relatively poor and the relatively rich segments of the population in the Latin American metropolitan area. The error bars in the curves for the random shuffling case correspond to the standard deviations, and all the other error bars correspond to the 95% confidence interval using a jackknife resampling technique as in (37).

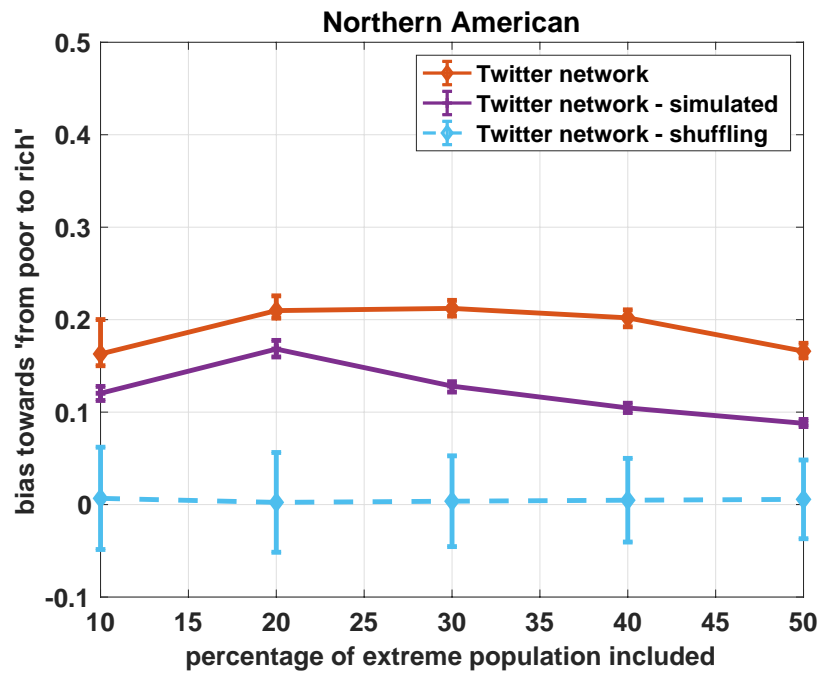


Figure S18: Asymmetry in the interaction patterns between the relatively poor and the relatively rich segments of the population in the Northern American metropolitan area. The error bars in the curves for the random shuffling case correspond to the standard deviations, and all the other error bars correspond to the 95% confidence interval using a jackknife resampling technique as in (37).

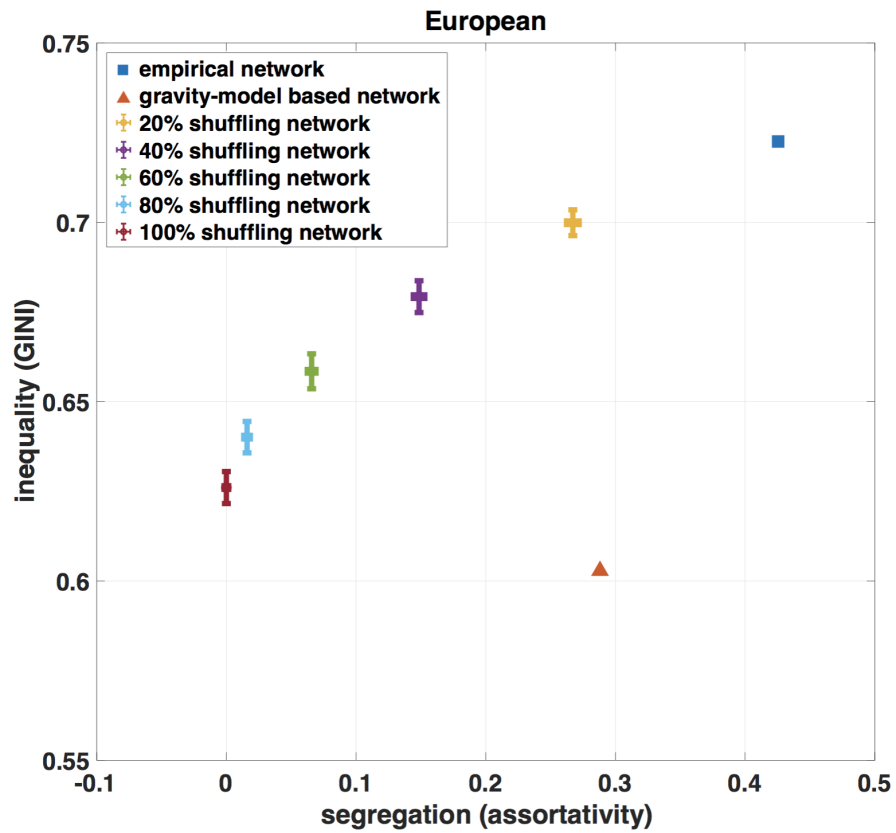


Figure S19: Association of segregation (assortativity) and inequality (GINI coefficient) between neighborhoods in terms of total sales income in the European metropolitan area. The error bars correspond to the standard deviations.

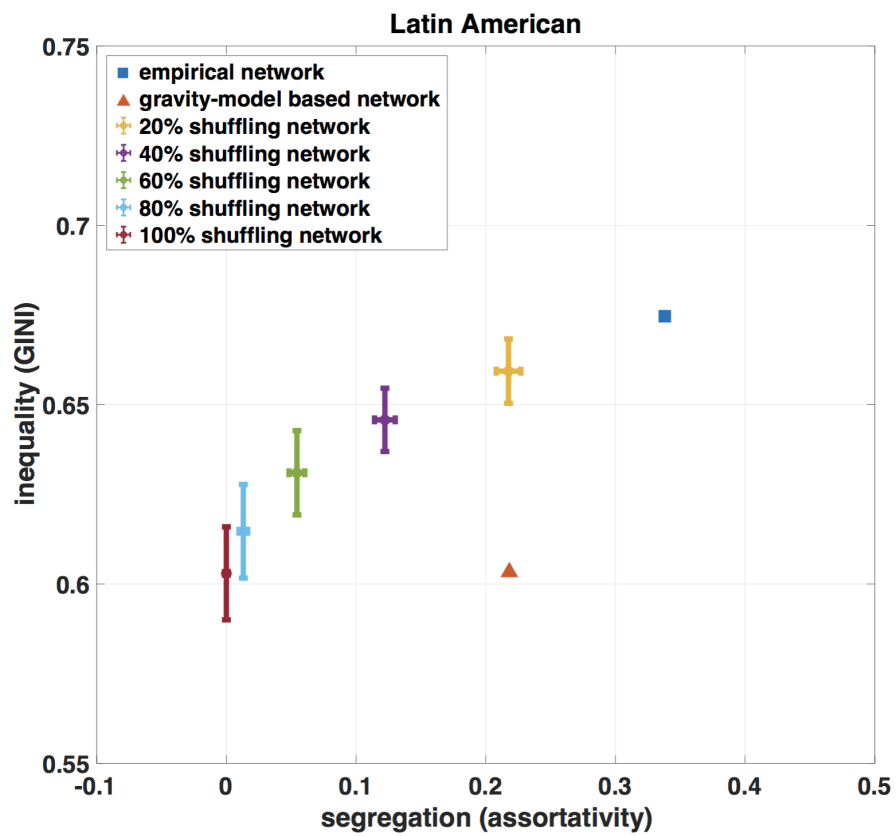


Figure S20: Association of segregation (assortativity) and inequality (GINI coefficient) between neighborhoods in terms of total sales income in the Latin American metropolitan area. The error bars correspond to the standard deviations.

Credit card data set		Twitter data set	
c_p	0.249	c_t	0.119
β_{p1}	0.762	β_{t1}	0.594
β_{p2}	0.598	β_{t2}	0.541
ϵ_p	0.233	ϵ_t	0.029
α_p	0.918	α_t	0.582

(a)

Credit card data set		Twitter data set	
c_p	0.231	c_t	0.085
β_{p1}	0.681	β_{t1}	0.493
β_{p2}	0.824	β_{t2}	0.829
ϵ_p	1.026	ϵ_t	0.298
α_p	1.058	α_t	0.633

(b)

Twitter data set	
c_t	7.941
β_{t1}	0.276
β_{t2}	0.353
ϵ_t	0.330
α_t	0.837

(c)

Table S1: Model parameters obtained by an OLS fitting, for the (a) European metropolitan area, (b) Latin American metropolitan area, and (c) Northern American metropolitan area.